

Formation of Light Isotopes by Protons and Deuterons of 3.65 GeV/nucleon on Separated Tin Isotopes

A. R. Balabekyan^{1,2}, A. S. Danagulyan¹, J. R. Drnoyan¹, G. H. Hovhannisyan¹, J. Adam^{2,3}, V. G. Kalinnikov², M. I. Krivopustov², V. S. Pronskikh², V. I. Stegailov², A. A. Solnyshkin², P. Chaloun^{2,3}, V. M. Tsoupko-Sitnikov²
S. G. Mashnik⁴, K. K. Gudima⁵

¹Yerevan State University, Armenia

²JINR, Dubna, Russia

³INF AS Rěz, Czech Republic

⁴Los Alamos National Laboratory, Los Alamos, NM 87545, USA

⁵Institute of Applied Physics, Academy of Science of Moldova, Chișinău

Abstract

We measure cross sections for residual nuclide formation in the mass range $7 \leq A \leq 96$ caused by bombardment with protons and deuterons of 3.65 GeV/nucleon energy of enriched tin isotopes (^{112}Sn , ^{118}Sn , ^{120}Sn , ^{124}Sn). The experimental data are compared with calculations by the codes FLUKA, LAHET, CEM03, and LAQGSM03. Scaling behavior is observed for the whole mass region of residual nuclei, showing a possible multifragmentation mechanism for the formation of light products ($7 \leq A \leq 30$). Our analysis of the isoscaling dependence also shows a possible contribution of multifragmentation to the production of heavier nuclides, in the mass region $40 \leq A \leq 80$.

1 Introduction

The nuclear reaction mechanism of fragmentation has been investigated for more than 60 years. A turning point in this study was marked by Jacobsson *et al.* in 1982, who measured multiple fragment production in nuclear emulsions containing Ag and Br, irradiated with ^{12}C at $55A$ and $110A$ MeV/nucleon [1]. These data stimulated development of new models to explain the formation of multiple fragments by a “liquid-gas” phase transition in hot nuclear matter (see, *e.g.*, [2, 3]).

The isospin dependence in the equation of state of nuclear matter is very important, being at the same time poorly known property of neutron-rich nuclear matter [4]. In recent years, much attention has been paid to the isospin dependence both in nucleus-nucleus experiments with an excess of neutrons in the bombarding and/or target nuclei and in experiments with different types of light projectiles on targets with different neutron/proton ratios [5]–[7]. Such investigations may help obtain information about the equation of state of the asymmetric nuclear matter.

Many experiments have been devoted to the study of nuclear multifragmentation, where several fragments in the mass region $3 \leq Z \leq 20$ are formed from hot nuclear matter [8, 9]. Observation of isoscaling, that is, the dependence of fragment formation probabilities on the third component of their isotopic spins, has increased the possibility of obtaining information on the formation mechanisms of these fragments [10]–[12]. Early work in this field was done by Bogatin *et al.* [13, 14] and has continued [15].

Recently experimentalists and theorists have focussed on the investigation of formation mechanisms of heavy fragments ($Z \geq 20$) by different projectiles (γ -rays, π^- -meson etc.) [5]–[7]. Experiments with a direct registration of heavy fragments do not provide a comprehensive understanding of fragments in this mass region. The induced-radioactivity method adds more possibilities and the investigation of mechanisms of heavy-fragment production becomes more realistic [16, 17].

The aim of the present work is to investigate the formation of product nuclei on separated tin isotopes by proton and deuteron beams of 3.65 GeV/nucleon in three mass regions of product nuclides: $7 \leq A \leq 30$, $40 \leq A \leq 80$, and $81 \leq A \leq 96$.

2 Experimental results and discussion

Targets of enriched tin isotopes ^{112}Sn , ^{118}Sn , ^{120}Sn , and ^{124}Sn are irradiated at the Nuclotron and Synchrophasotron of the LHE JINR in Dubna by proton and deuteron beams with energy of 3.65 GeV/nucleon. The description of the experiment is given in [18]. The measurement of products in the mass range $7 \leq A \leq 80$ is performed by studying the induced activity. The radioactive nuclei obtained are identified by the characteristic γ -rays and their half-lives. For beam monitoring, we employ the reactions $^{27}\text{Al}(d, 3p2n)^{24}\text{Na}$ and $^{27}\text{Al}(p, 3pn)^{24}\text{Na}$, whose cross sections are taken as of 14.2 ± 0.2 mb [19] and 10.6 ± 0.8 mb [20], respectively. Cross sections for about 70 products from each target for the proton and deuteron beams are obtained. The measured cross sections of all products are shown in Tables 1 and 2: index “I” denotes independent yields while “C” indicates cumulative ones.

Table 1. Measured product cross sections for $p + ^{112,118,120,124}\text{Sn}$

Product	Type	Cross section (mb)			
		^{112}Sn	^{118}Sn	^{120}Sn	^{124}Sn
^7Be	I	13.9 ± 1.5	9.4 ± 0.3	8.2 ± 1.4	7.5 ± 0.8
^{22}Na	C	2.3 ± 0.3	2.4 ± 0.4	2.1 ± 0.4	1.7 ± 0.2
^{24}Na	C	3.25 ± 0.3	3.23 ± 0.2	3.69 ± 0.3	3.97 ± 0.3
^{28}Mg	C	0.39 ± 0.06	0.53 ± 0.05	0.75 ± 0.08	0.89 ± 0.07
^{38}Cl	I		1.67 ± 0.2	1.5 ± 0.2	
^{39}Cl	C		0.57 ± 0.02	0.34 ± 0.07	
^{42}K	C	1.76 ± 0.11	1.85 ± 0.25	1.95 ± 0.2	2.1 ± 0.2
^{43}K	C	0.74 ± 0.06	0.85 ± 0.08	1.04 ± 0.1	1.32 ± 0.1
^{43}Sc	C	0.72 ± 0.18	0.6 ± 0.2	0.45 ± 0.2	0.2 ± 0.03
^{44g}Sc	I	0.97 ± 0.09	0.54 ± 0.15	0.58 ± 0.04	0.36 ± 0.09
^{44m}Sc	I	2.28 ± 0.1	1.45 ± 0.06	1.4 ± 0.07	1.7 ± 0.1
^{46}Sc	I	2.2 ± 0.2	2.35 ± 0.2	2.6 ± 0.4	2.4 ± 0.2
^{48}Sc	I	0.3 ± 0.05	0.38 ± 0.07	0.42 ± 0.05	0.7 ± 0.09
^{48}Cr	C	0.19 ± 0.07	0.1 ± 0.01	0.13 ± 0.04	
^{51}Cr	C		3.7 ± 0.6	3.3 ± 0.6	
^{48}V	I	2.7 ± 0.15	1.68 ± 0.1	1.76 ± 0.1	1.06 ± 0.1
^{52}Mn	C	1.9 ± 0.04	1.12 ± 0.03	1.03 ± 0.04	0.7 ± 0.08
^{54}Mn	I	6.1 ± 0.3	5.1 ± 0.25	4.8 ± 0.3	4.2 ± 0.3
^{56}Mn	C	0.8 ± 0.03	1.08 ± 0.07	1.33 ± 0.1	1.86 ± 0.08
^{59}Fe	C	0.37 ± 0.05	0.83 ± 0.09	0.85 ± 0.07	1.17 ± 0.1

Table 1 (continued)

Product	Type	Cross section (mb)			
		^{112}Sn	^{118}Sn	^{120}Sn	^{124}Sn
^{56}Co	C	1.8 ± 0.1	1.7 ± 0.2	1.75 ± 0.2	1.54 ± 0.2
^{58}Co	C	5.7 ± 0.4	4.8 ± 0.5	4.8 ± 0.4	3.6 ± 0.4
^{67}Cu	C	0.1 ± 0.02	0.29 ± 0.05	0.44 ± 0.04	0.52 ± 0.05
^{65}Zn	C	9.1 ± 0.3	6.9 ± 0.3	6.9 ± 0.3	5.1 ± 0.3
^{66}Ga	C	4.8 ± 0.4	3.1 ± 0.2	2.9 ± 0.3	2.5 ± 0.3
^{67}Ga	C	8.9 ± 0.07	6.7 ± 0.4	6.4 ± 0.4	5.3 ± 0.5
^{69}Ge	C	7.5 ± 0.7	5.3 ± 0.5	5.0 ± 0.3	3.9 ± 0.5
^{77}Ge	C		0.2 ± 0.05	0.16 ± 0.05	
^{70}As	C	3.0 ± 0.5	1.9 ± 0.5	1.42 ± 0.2	2.1 ± 0.6
^{71}As	C	8.01 ± 0.8	5.54 ± 0.06	5.3 ± 0.4	4.1 ± 0.5
^{72}As	C	2.8 ± 0.4	2.1 ± 0.3	1.9 ± 0.4	2.1 ± 0.6
^{74}As	I	1.92 ± 0.15	2.6 ± 0.3	3.07 ± 0.4	3.5 ± 0.25
^{76}As	I	4.5 ± 0.4	5.1 ± 0.4	5.3 ± 0.5	6.3 ± 0.4
^{73}Se	C	5.7 ± 0.15	3.8 ± 0.15	3.5 ± 0.15	2.4 ± 0.2
^{75}Se	C	13.2 ± 0.5	10.3 ± 0.7	10.1 ± 1.0	8.8 ± 0.7
^{76}Br	C	10.5 ± 1	7.3 ± 0.5	6.6 ± 0.7	5.2 ± 0.4
^{77}Br	I	10.4 ± 0.4	8.4 ± 0.2	8.4 ± 0.2	7.8 ± 0.2
^{82}Br	I		0.26 ± 0.04	0.25 ± 0.02	0.49 ± 0.03
^{76}Kr	C	1.6 ± 0.2	1.03 ± 0.05	0.9 ± 0.07	0.55 ± 0.05
^{77}Kr	C		3.2 ± 0.3	2.7 ± 0.3	1.76 ± 0.16
^{81}Rb	C	16.4 ± 0.6	11.7 ± 0.2	11.5 ± 0.4	8.8 ± 0.6
^{82m}Rb	I	5.2 ± 0.05	5.3 ± 0.4	5.9 ± 0.4	5.7 ± 0.3
^{83}Rb	C	18.6 ± 0.7	15.3 ± 0.5	16.0 ± 0.6	13.8 ± 0.3
^{84g}Rb	I	1.4 ± 0.3	2.3 ± 0.2	2.8 ± 0.2	4.4 ± 0.6
^{86}Rb	I	0.34 ± 0.09		1.09 ± 0.14	1.85 ± 0.24
^{83}Sr	C	14.6 ± 0.1	10.3 ± 0.3	9.8 ± 0.2	7.4 ± 0.5
^{85}Sr	C	21 ± 1.6	17.5 ± 1.7	17.3 ± 1.5	15.2 ± 0.9
^{84m}Y	I	5.1 ± 0.5	3.4 ± 0.3	2.6 ± 0.4	2.1 ± 0.4
^{86m}Y	I	4.9 ± 0.4	6.4 ± 0.1	6.7 ± 0.4	5.5 ± 0.4
^{87m}Y	C	18.6 ± 0.7	15.5 ± 0.9	15.8 ± 0.3	12.8 ± 0.4
^{87g}Y	I	4.3 ± 0.4	3.5 ± 0.3	4.0 ± 0.3	2.8 ± 0.2
^{86}Zr	C	8.8 ± 0.5	4.8 ± 0.15	3.5 ± 0.1	2.3 ± 0.25
^{88}Zr	C	20.2 ± 2.0	13.8 ± 0.8	14.4 ± 1.0	10.2 ± 0.9
^{89}Zr	C	20.2 ± 0.5	16.35 ± 0.3	16.4 ± 0.3	13.1 ± 0.7
^{90}Nb	C	18.2 ± 1.0	12.4 ± 0.4	11.6 ± 1.2	8.6 ± 0.4
^{95g}Nb	C		0.8 ± 0.03	1.75 ± 0.07	2.40 ± 0.25
^{95m}Nb	I		0.17 ± 0.08	0.35 ± 0.06	
^{96}Nb	I	0.33 ± 0.08	0.42 ± 0.07	0.65 ± 0.06	1.14 ± 0.16
^{90}Mo	C	5.9 ± 0.2	2.6 ± 0.3	2.1 ± 0.3	1.1 ± 0.1
^{93m}Mo	I	3.5 ± 0.2	4.1 ± 0.4	4.4 ± 0.3	3.8 ± 0.2
^{99}Mo	C	0.19 ± 0.02	0.26 ± 0.02	0.62 ± 0.13	1.65 ± 0.25
^{93}Tc	C	12.35 ± 0.8	6.95 ± 0.3	5.7 ± 0.5	3.4 ± 0.3

Table 1 (continued)

Product	Type	Cross section (mb)			
		^{112}Sn	^{118}Sn	^{120}Sn	^{124}Sn
^{94}Tc	I	9.8 ± 0.2	6.5 ± 0.1	6.7 ± 0.2	4.4 ± 0.3
^{95g}Tc	I	12.4 ± 0.6	9.8 ± 0.4	8.3 ± 0.3	7.5 ± 0.3
^{95m}Tc	I	1.0 ± 0.1	1.1 ± 0.1	0.8 ± 0.08	0.56 ± 0.10
^{96}Tc	I	4.4 ± 0.1	6.7 ± 0.2	7.4 ± 0.25	6.4 ± 0.1

Table 2. Measured product cross sections for d + $^{112,118,120,124}\text{Sn}$

Product	Type	Cross section (mb)			
		^{112}Sn	^{118}Sn	^{120}Sn	^{124}Sn
^7Be	I	31.1 ± 2.7		25.5 ± 2.5	23.1 ± 4.0
^{22}Na	C	23.3 ± 0.4	8.1 ± 1.5	4.1 ± 0.1	3.5 ± 0.9
^{24}Na	C	6.2 ± 0.4	10.0 ± 1.3	9.9 ± 0.8	12.2 ± 1.1
^{28}Mg	C	1.0 ± 0.1	1.8 ± 0.1	1.6 ± 0.2	2.9 ± 0.8
^{38}S	C			0.37 ± 0.04	0.56 ± 0.06
^{38}Cl	I			3.0 ± 0.2	3.5 ± 0.5
^{39}Cl	C			1.1 ± 0.1	1.8 ± 0.6
^{42}K	C	2.4 ± 0.2	4.5 ± 1.2	3.9 ± 0.5	5.2 ± 0.5
^{43}K	C	1.2 ± 0.1	2.4 ± 0.4	2.1 ± 0.3	3.1 ± 0.3
^{43}Sc	C	1.2 ± 0.1	1.4 ± 0.02	1.4 ± 0.1	2.1 ± 0.1
^{44m}Sc	I	2.9 ± 0.1	3.2 ± 0.4	2.7 ± 0.7	2.0 ± 0.3
^{44g}Sc	I	1.7 ± 0.4	2.0 ± 0.3	1.5 ± 0.2	1.5 ± 0.2
^{46}Sc	I	3.3 ± 0.8	6.1 ± 0.8	6.1 ± 0.3	6.6 ± 0.3
^{47}Sc	C	3.5 ± 0.2			
^{48}Sc	I	0.5 ± 0.1	1.0 ± 0.09	1.1 ± 0.2	1.6 ± 0.3
^{48}V	C	3.5 ± 0.3	3.5 ± 0.4	3.2 ± 0.1	2.9 ± 0.5
^{51}Cr	C	14.1 ± 1.4	6.1 ± 0.4	7.4 ± 0.8	5.7 ± 0.5
^{52g}Mn	C	2.3 ± 0.4	2.1 ± 0.2	2.0 ± 0.4	1.5 ± 0.3
^{56}Mn	C	2.4 ± 0.6	3.1 ± 0.4	2.9 ± 0.1	4.3 ± 0.3
^{59}Fe	C	0.68 ± 0.03	1.5 ± 0.2	1.7 ± 0.1	2.7 ± 0.2
^{55}Co	C	0.35 ± 0.05			
^{56}Co	C	1.9 ± 0.1	1.9 ± 0.3	1.4 ± 0.1	1.1 ± 0.1
^{57}Co	C	6.9 ± 0.2	11.8 ± 0.3	5.9 ± 0.2	4.8 ± 0.1
^{58}Co	I	8.3 ± 0.3	9.9 ± 0.2	7.6 ± 1.0	7.8 ± 0.5
^{60}Cu	C	1.9 ± 0.4	1.04 ± 0.19	1.7 ± 0.1	0.5 ± 0.09
^{67}Cu	C			0.34 ± 0.04	0.34 ± 0.01
^{62}Zn	C	1.25 ± 0.05			0.3 ± 0.03
^{65}Zn	C	16.5 ± 1.0		10.7 ± 0.2	10.1 ± 0.4
^{69m}Zn	I	0.39 ± 0.05	0.84 ± 0.05	1.1 ± 0.1	1.4 ± 0.1
^{66}Ga	C	5 ± 0.5		3.3 ± 0.3	3.4 ± 0.3
^{67}Ga	C	8.6 ± 0.3	9.7 ± 1.3	9.3 ± 0.7	8.7 ± 0.3
^{73}Ga	C	0.48 ± 0.12			

Table 2 (continued)

Product	Type	Cross section (mb)			
		^{112}Sn	^{118}Sn	^{120}Sn	^{124}Sn
^{69}Ge	C	6.2 ± 0.6	8.8 ± 1.6	7.2 ± 0.5	6.7 ± 0.9
^{77}Ge	C			1.3 ± 0.1	2.5 ± 0.3
^{71}As	C	7.4 ± 0.2	7.73 ± 0.8	6.7 ± 0.2	5.4 ± 0.4
^{74}As	I	2.1 ± 0.1	2.65 ± 0.5	4.3 ± 0.1	6.9 ± 0.8
^{78}As	C	1.35 ± 0.05			0.9 ± 0.2
^{73g}Se	C	6.6 ± 0.1	6.4 ± 0.4	5.2 ± 0.6	4.3 ± 0.3
^{75}Se	I	7.0 ± 0.77	9.4 ± 1.49	10.8 ± 0.93	10.3 ± 1.06
^{75}Br	C	6.8 ± 0.6	5.4 ± 0.5	4.4 ± 0.3	3.5 ± 0.3
^{77}Br	I	4.5 ± 0.55	6.9 ± 1.18	6.0 ± 0.47	6.4 ± 0.74
^{77}Kr	C	5.2 ± 0.6	3.5 ± 0.5	3.5 ± 0.2	2.4 ± 0.2
^{79}Kr	I	1.2 ± 0.13		8.9 ± 1.22	8.0 ± 1.01
^{79}Rb	C	10.1 ± 1.0		2.8 ± 0.3	1.9 ± 0.2
^{81}Rb	C	14.1 ± 0.7	15.7 ± 0.6	12.8 ± 0.4	10.9 ± 0.7
^{83}Rb	C	20.3 ± 0.8	24.15 ± 0.95	21.7 ± 1.0	21.6 ± 0.6
^{84}Rb	I	1.2 ± 0.1	3.2 ± 0.3	4.1 ± 0.5	6.4 ± 0.3
^{82}Sr	C	10.1 ± 1.5	8.8 ± 1.5	6.0 ± 0.6	4.6 ± 0.5
^{83}Sr	C	13.1 ± 0.3	13.7 ± 1.2	10.3 ± 1.3	9.0 ± 0.6
^{85}Sr	I			13.3 ± 1.55	15.9 ± 1.4
^{85m}Y	C			7.7 ± 0.9	3.5 ± 0.3
^{85g}Y	C				2.9 ± 0.7
^{86m}Y	I	5.0 ± 0.3	8.3 ± 0.2	7.6 ± 0.1	6.6 ± 0.2
^{86g}Y	I	6.5 ± 0.5		8.9 ± 0.1	8.8 ± 0.8
^{87g}Y	C	20.5 ± 2.1		20.0 ± 2.0	19.3 ± 2.0
^{88}Y	I		10.2 ± 1.7	5.6 ± 0.5	7.8 ± 0.8
^{86}Zr	C	7.4 ± 0.2	5.4 ± 0.1	3.7 ± 0.3	2.8 ± 0.1
^{88}Zr	C	18.4 ± 2.2		16.8 ± 0.2	14.6 ± 0.2
^{89}Zr	C	18.4 ± 0.4		17.8 ± 0.5	16.9 ± 0.7
^{93m}Tc	I	10.1 ± 0.6		6.6 ± 0.5	2.0 ± 0.2
^{94m}Tc	I	9.5 ± 1.0			5.6 ± 0.2
^{94g}Tc	I	4.3 ± 0.3	1.9 ± 0.46		2.4 ± 0.8
^{95m}Tc	I		15.1 ± 0.7		
^{95g}Tc	I	1.23 ± 0.05	1.23 ± 0.07	1.2 ± 0.2	1.0 ± 0.1
^{96g}Tc	I	4.4 ± 0.3	9.1 ± 0.6		8.4 ± 1.3

To reveal the production mechanisms of light nuclei, the experimental results are analyzed from the viewpoint of:

- 1) exponential dependence of cross sections on the mass and charge numbers;
- 2) including isospin dependence.

Investigations by many authors have showed that the yields of fragments from various nuclear reactions can be represented as $\sigma(A_f) \sim A_f^{-\tau}$ and $\sigma(Z_f) \sim Z_f^{-\tau}$, where τ has values of about 1.5–2 depending on the reactions, where A_f and Z_f are the mass and charge numbers of the fragments. Note that calculations by the Statistical Multifragmentation Model (SMM) [3] for the mass region of fragments discussed here provide an exponential dependence with

$\tau = 2.2$.

The isospin dependence of the available experimental yields points to an isoscaling behavior. In the case of multifragmentation, the ratio of the yields of fragments produced from different targets has an exponential dependence on the number of protons and neutrons of the product isotopes described by the formula [10]:

$$R_{21}(t_3) = Y_2(N, Z)/Y_1(N, Z) = C \exp(\alpha N + \beta Z), \quad (1)$$

where $Y(N, Z)$ is the yield of fragment with Z protons and N neutrons, and $t_3 = (N - Z)/2$ is the third projection of the fragment isospin. Indices 1 and 2 correspond to different targets with different isotopic compositions, with 2 corresponding to the more neutron-rich target and where C is a normalization parameter. In Ref. [11], the parameters α and β were expressed using the difference of chemical potentials of the two systems as following: $\alpha = \Delta\mu_n/T$, $\beta = \Delta\mu_p/T$, where T is the temperature of the excited nucleus.

Since in our measurements we use targets of different isotopes of the same element, we analyze our data with the following formula:

$$R_{21}(t_3) = Y_2(N, Z)/Y_1(N, Z) = \exp(C + Bt_3), \quad (2)$$

where C and B are fitting parameters [17]. The parameter B is related to the difference of the chemical potentials of protons and neutrons in the fragment and depends on the temperature of the excited nucleus; therefore it may reveal information about the formation mechanism of the corresponding product.

Figure 1 shows the dependence of Y_2/Y_1 on t_3 for the entire mass region of product nuclei from proton-induced reactions for different values of the difference in the neutron numbers of considered pairs of targets ΔN . Similar dependences for deuteron-induced reactions are shown in Figure 2. In both these figures, symbols show the measured data while lines show their fit with formula (2).

Tables 3 and 4 present the values of the fitting parameter B for different combinations of targets pairs and for different mass regions of product nuclei for proton- and deuteron-induced reactions, respectively. Figure 3 shows the dependence of the parameter B on the difference of neutron numbers in a pair of targets, ΔN , for different mass regions of products from proton-induced reactions.

The value of the parameter B increases linearly with increasing ΔN . B also increases with increasing mass of the product nuclei. The dependence of parameter B on the difference of the neutron numbers in a pair of targets, ΔN , is fitted using the following formula:

$$B = k + d\Delta N, \quad (3)$$

where $k = -0.036 \pm 0.01$ and $d = 0.094 \pm 0.016$ for the mass region $7 \leq A \leq 30$, $k = -0.0008 \pm 0.0001$ and $d = 0.071 \pm 0.005$ for the mass region $40 \leq A \leq 80$, and $k = -0.113 \pm 0.060$ and $d = 0.033 \pm 0.008$ for the mass region $A \geq 80$. The value of the parameter d changes with the mass number of the products, and could be a factor in understanding the formation mechanism of the final nuclides.

From Tables 3 and 4, we see that for the production of $^{93-96}\text{Tc}$ and $^{81-86}\text{Rb}$ on the pair of targets $^{124}\text{Sn}/^{112}\text{Sn}$, the parameter B has values of 1.07 ± 0.32 and 0.94 ± 0.20 for proton-induced reactions and 1.10 ± 0.40 and 1.17 ± 0.29 for deuteron-induced reactions, respectively. This agrees with similar values of B of 1.22 ± 0.12 and 1.23 ± 0.13 found in the literature for such products at a higher energy of 8.1 GeV [17]. This allows us to conclude that residual products in this mass region are produced via spallation processes of successive particle evaporation.

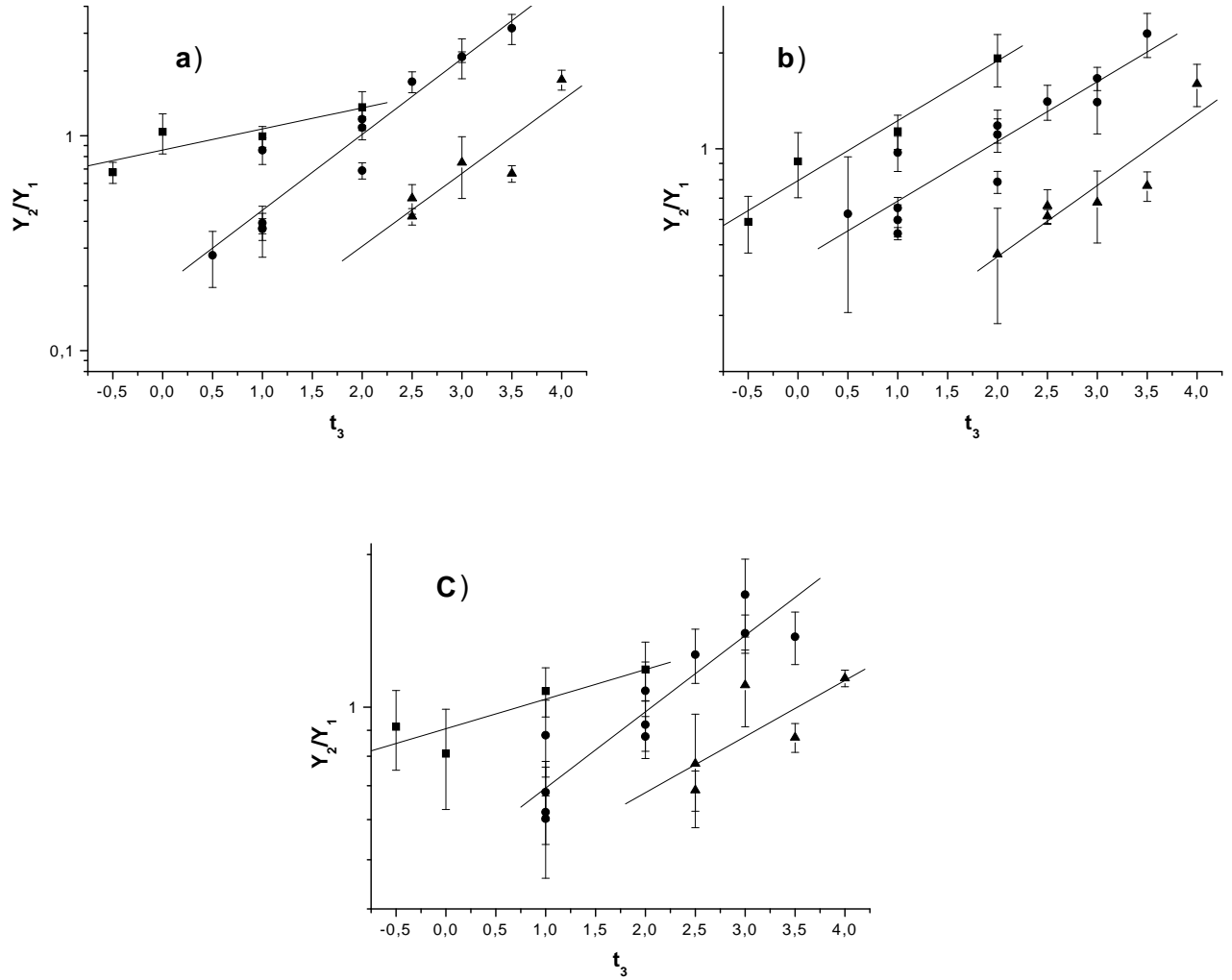


Figure 1: Ratio $R_{21}(t_3) = Y_2/Y_1$ versus the isotopic-spin projection t_3 of products for different target pairs bombarded by protons: a) for $\Delta N=12$ (target pairs $^{124}\text{Sn}/^{112}\text{Sn}$); b) for $\Delta N=8$ (target pairs $^{120}\text{Sn}/^{112}\text{Sn}$); and c) for $\Delta N=4$ (target pairs $^{124}\text{Sn}/^{120}\text{Sn}$). Symbols show measured yields of different products as following: ■ — for the mass region $7 \leq A \leq 30$; ● — for the mass region $40 \leq A \leq 60$; and ▲ — for the mass region $70 \leq A \leq 80$. Lines are results of fitting the data with formula (2).

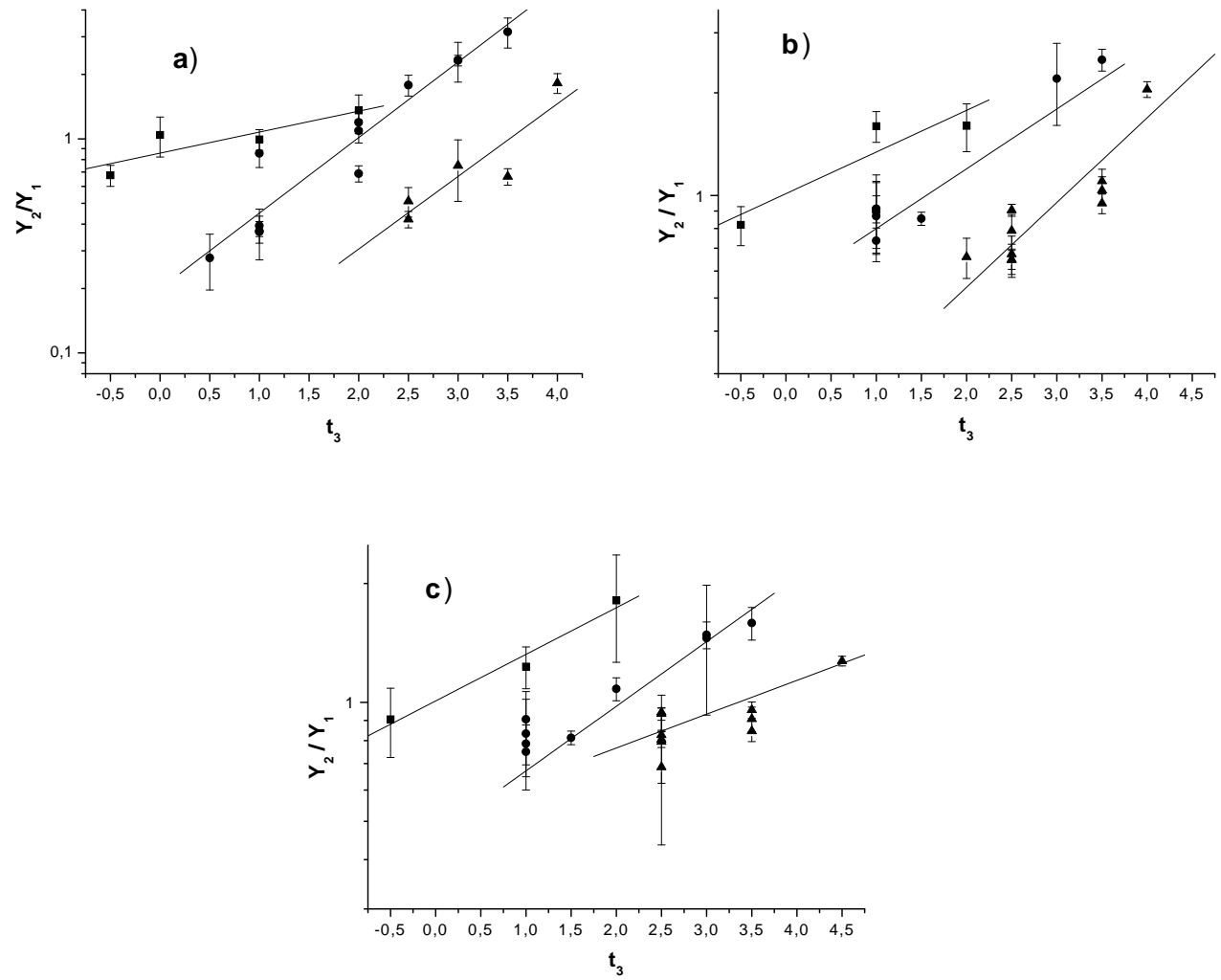


Figure 2: The same as in Fig. 1, but for deuteron-induced reactions.

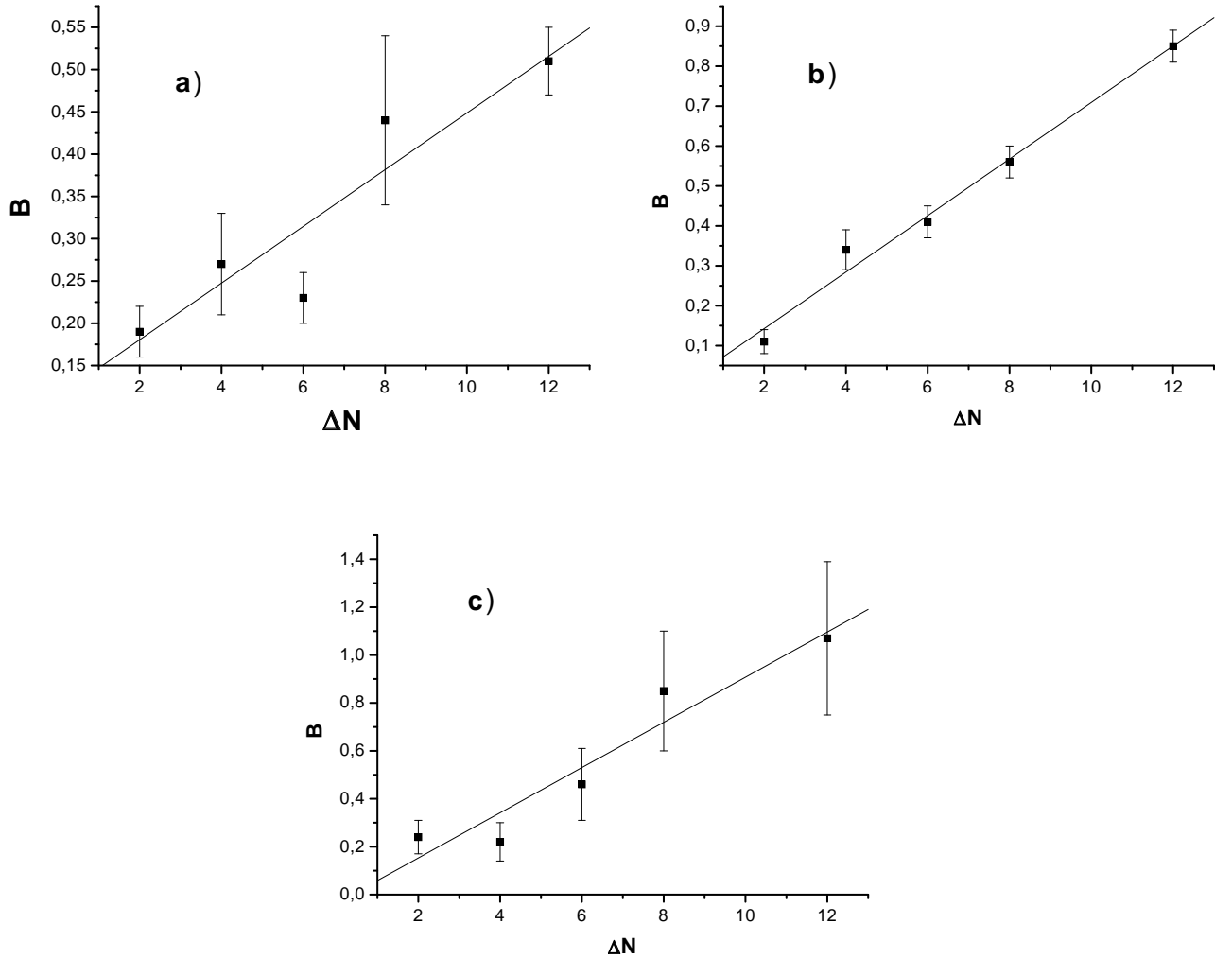


Figure 3: Parameter B versus the difference in the excess of neutron number (ΔN) of targets for proton-induced reactions. Symbols show values obtained by fitting the experimental data with Eq. (2) as following: a) for the product mass region $7 \leq A \leq 30$; b) for the mass region $40 \leq A \leq 80$; and c) for the mass region $A \geq 80$. Lines are results of fitting the parameter B with formula (3).

Table 3. Mean values of the fitting parameter B for different target pairs (with the difference in the excess neutron number of ΔN) bombarded by protons

Product nuclei	$\Delta N = 2$	$\Delta N = 4$	$\Delta N = 6$	$\Delta N = 8$	$\Delta N = 12$
$7 \leq A \leq 30$	0.19 ± 0.03	0.27 ± 0.06	0.23 ± 0.03	0.44 ± 0.10	0.51 ± 0.04
$40 \leq A \leq 60$	0.11 ± 0.03	0.34 ± 0.05	0.41 ± 0.04	0.56 ± 0.04	0.85 ± 0.04
$70 \leq A \leq 80$	0.18 ± 0.05	0.25 ± 0.13	0.36 ± 0.09	0.51 ± 0.10	0.78 ± 0.21
$^{81-86}\text{Rb}$	0.25 ± 0.02	0.32 ± 0.04	0.66 ± 0.02	0.62 ± 0.15	0.94 ± 0.20
$^{93-96}\text{Tc}$	0.24 ± 0.07	0.22 ± 0.08	0.46 ± 0.15	0.85 ± 0.25	1.07 ± 0.32

Table 4. The same as in Table 3, but for deuteron-induced reactions

Product nuclei	$\Delta N = 4$	$\Delta N = 6$	$\Delta N = 8$	$\Delta N = 12$
$7 \leq A \leq 30$	0.27 ± 0.05	0.26 ± 0.05	0.28 ± 0.12	0.55 ± 0.07
$40 \leq A \leq 60$	0.38 ± 0.1	0.41 ± 0.09	0.41 ± 0.10	0.78 ± 0.14
$70 \leq A \leq 80$	0.19 ± 0.07	0.5 ± 0.1	0.57 ± 0.14	0.77 ± 0.19
$^{81-86}\text{Rb}$	0.30 ± 0.08		0.87 ± 0.22	1.17 ± 0.29
$^{93-96}\text{Tc}$	0.15 ± 0.08	0.48 ± 0.30	0.51 ± 0.07	1.10 ± 0.40

On the other hand, much smaller values of the fitting parameter B in the mass region $7 \leq A \leq 30$ may point to a possible multifragmentation mechanism in the formation of these light fragments [17, 10].

A different situation may be seen in the mass region $40 \leq A \leq 60$, both for proton- and deuteron-induced reactions. The values of B in this mass region is generally lower than for the heavy products $^{81-86}\text{Rb}$ and $^{93-96}\text{Tc}$, but higher than for light fragments with $7 \leq A \leq 30$. This may be understood if we assume that intermediate-mass nuclei are produced not only via evaporation of particles (the spallation mechanism) but also include a contribution from multifragmentation processes. This assumption is in agreement with results of our earlier studies [16] at bombarding proton energies of 0.66, 1.0, and 8.1 GeV: We found that an observed increase in the measured yields of intermediate-mass products can be described in the frameworks of the Intra-Nuclear Cascade (INC) model merged with SMM [3], *i.e.*, by the INC+SMM model, which considers a contribution of multifragmentation to the formation of such intermediate-mass nuclei.

In the present work, we compare the measured cross sections with predictions by the FLUKA [21], LAHET [22], CEM03 [23], and LAQGSM03 [23] codes (none of them considers the multifragmentation mechanism of fragment production). The first three codes are only applied to the proton-induced reactions, while LAGQSM03 is used for both protons and deuterons. In order to compare the measured cumulative cross sections with calculations, the corresponding theoretical cumulative yields were estimated from the calculated independent cross sections.

Figures 4, 5, and 6 show dependencies of ratios of theoretical to experimental cross sections as functions on the product mass numbers for deuteron- and proton-induced reaction, respectively. We see that, as a rule, all models describe most of the measured cross sections of heavy and medium products within a factor of two. Except for the CEM03 code, the agreement with the measured yields of light fragments is much worse, where the other codes underestimate some measured cross sections by up to two orders of magnitude and more. This could be related to the fact that all the models used here do not consider multifragmentation. But it is also true that they do not include simpler fission/fragmentation production mechanisms, either.

To have a better overall quantitative comparison of experimental data with calculations, we have analyzed our data using the mean deviation factor method suggested first by R. Michel [24]:

$$\langle F \rangle = 10^{\sqrt{\langle (\log[\sigma^{cal}/\sigma^{exp}])^2 \rangle}}, \quad (4)$$

with its standard deviation

$$S(\langle F \rangle) = 10^{\sqrt{\langle (|\log(\sigma^{cal}/\sigma^{exp})| - \log(\langle F \rangle))^2 \rangle}}, \quad (5)$$

where $\langle \rangle$ stands for averaging over all the products included in the comparison.

Values of the average deviation factor $\langle F \rangle$ and its standard deviation $S(\langle F \rangle)$ are listed in Table 5 for deuteron-induced reactions and in Table 6 for reactions with protons, respectively.

Table 5. Mean deviations of product yields calculated by LAQGSM03 from the measured data (parameters $\langle F \rangle \pm S(\langle F \rangle)$) for deuteron-induced reactions averaged over all compared cross sections

	^{112}Sn	^{118}Sn	^{120}Sn	^{124}Sn
$\langle F \rangle \pm S(\langle F \rangle)$	3.305 ± 3.08	2.04 ± 1.69	2.96 ± 2.75	2.41 ± 2.75

Table 6. Mean deviations of theoretical product yields from the measured data (parameters $\langle F \rangle \pm S(\langle F \rangle)$) for proton-induced reactions averaged over all compared cross sections

Models used	^{112}Sn	^{118}Sn	^{120}Sn	^{124}Sn
LAHET	4.07 ± 2.77	3.49 ± 2.40	3.37 ± 2.31	3.61 ± 2.56
FLUKA	5.92 ± 4.18	7.84 ± 5.19	8.87 ± 5.42	6.97 ± 4.29
LAQGSM03	5.10 ± 3.86	3.44 ± 2.62	3.09 ± 2.22	3.16 ± 2.14
CEM03	3.66 ± 3.02	3.26 ± 2.79	4.04 ± 3.29	3.60 ± 3.01

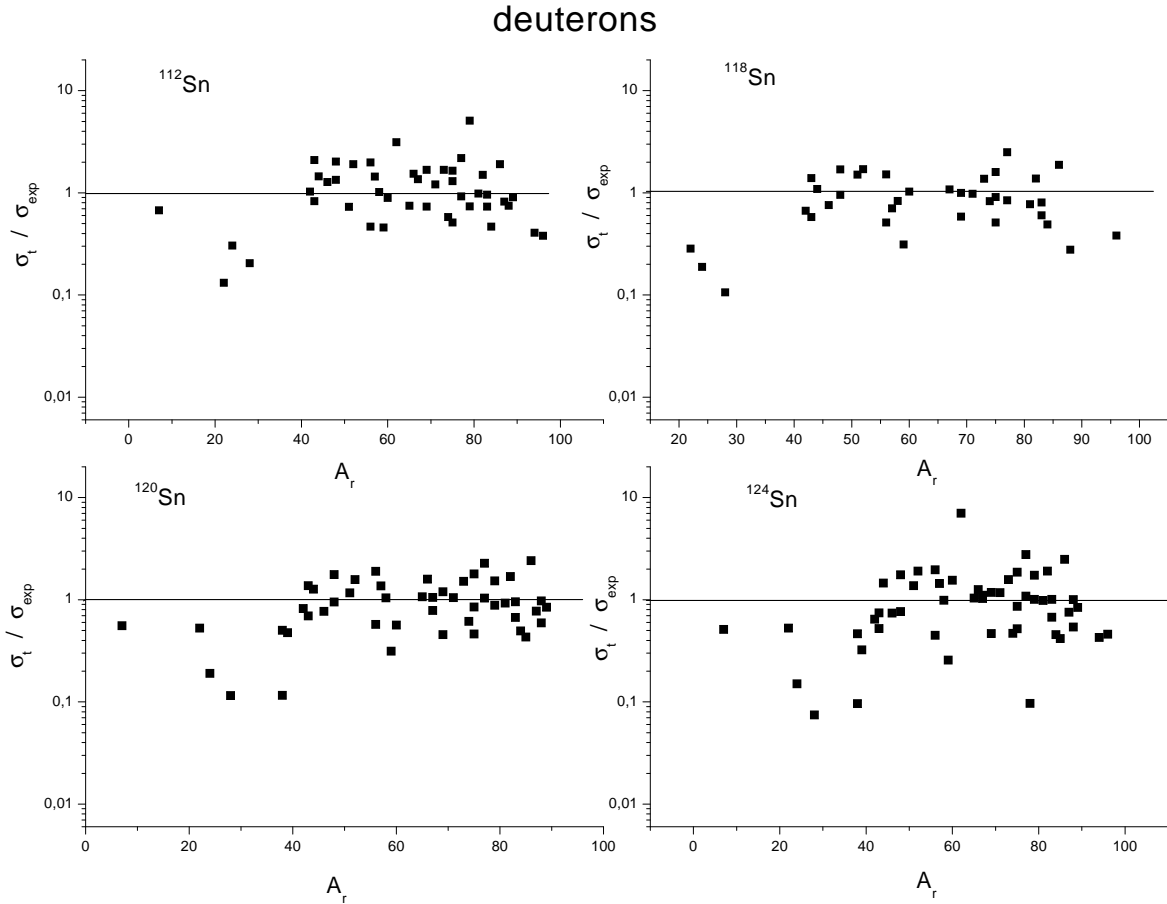
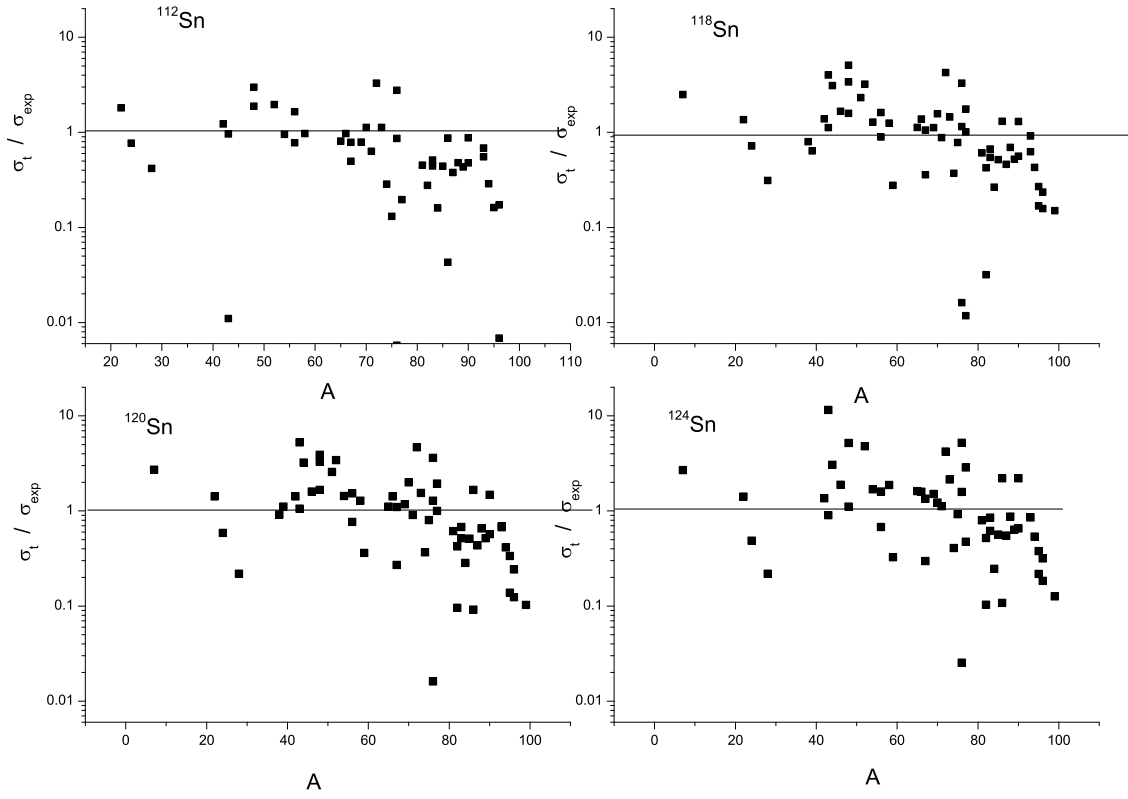


Figure 4: Dependence of the ratio of predicted by LAQGSM03 and experimental cross-sections on the mass number of products for deuteron-induced reactions.

CEM03



FLUKA

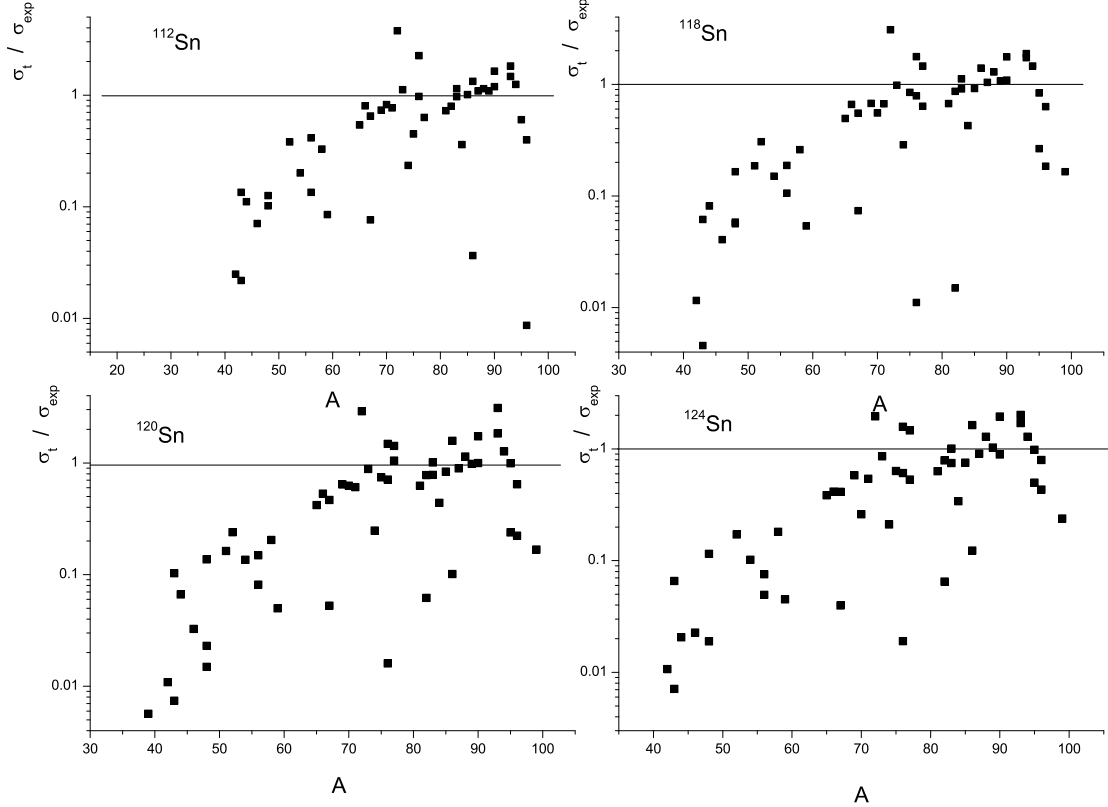
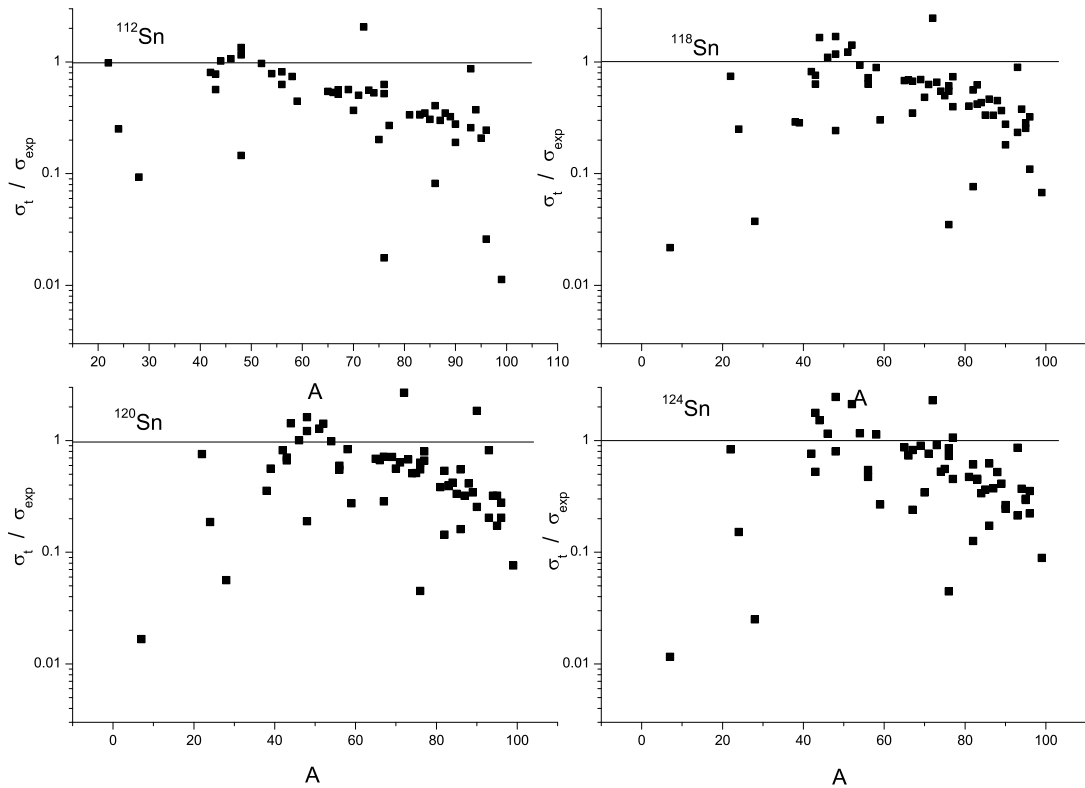


Figure 5: Dependences of ratios of predictions by CEM03 and FLUKA and experimental cross-sections on the mass number of products for proton-induced reactions.

LAHET



LAQGSM03

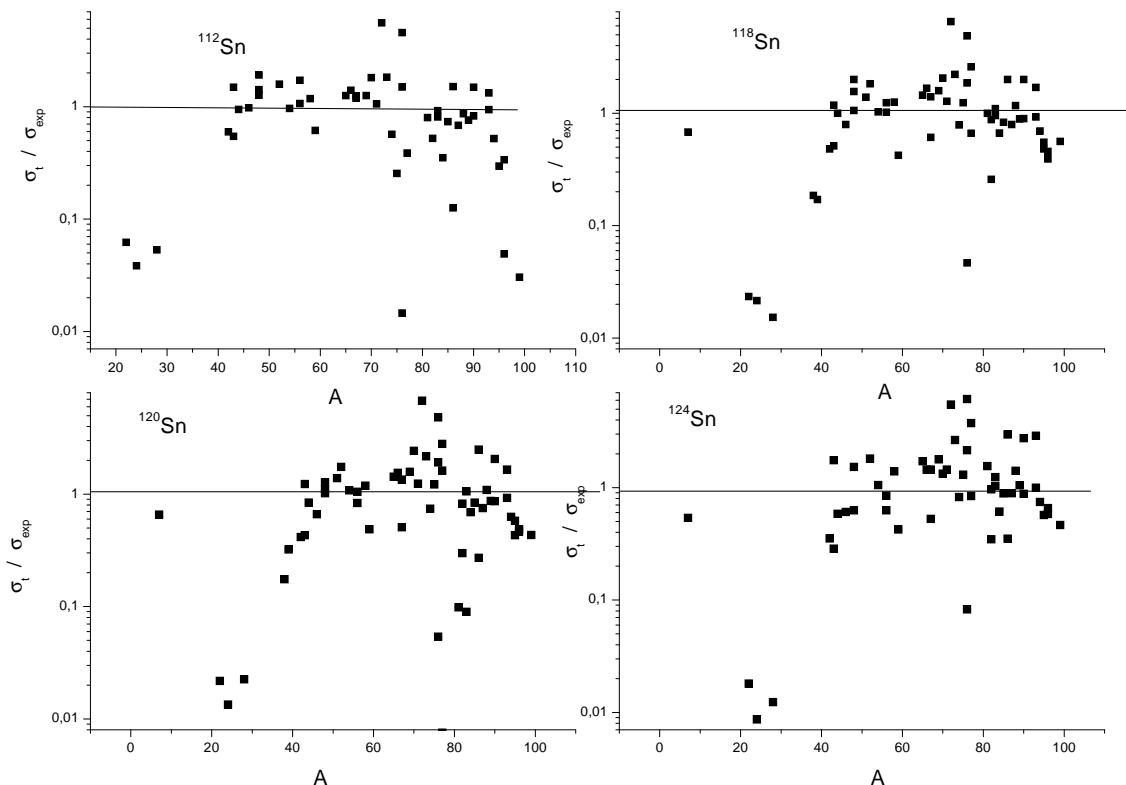


Figure 6: The same as in Fig. 5, but for LAHET and LAQGSM03.

The present analysis points to a possible formation of light nuclides via multifragmentation, which would suggest a “liquid-gas” phase transition taking place in hot nuclear matter formed by irradiation of target nuclei with high-energy particles. The intermediate-mass products are probably formed mainly via evaporation, but some contribution from multifragmentation is also possible, according to our study.

Acknowledgments

We thank Dr. A. J. Sierk for useful discussions and help. The work was partially supported by the Advanced Simulation Computing (ASC) Program at the Los Alamos National Laboratory operated by the University of California for the U. S. Department of Energy and by the Moldovan-US Bilateral Grants Program, CRDF Project MP2-3045-CH-02 and the NASA ATP01 Grant NRA-01-01-ATP-066.

References

- [1] B. Jacobsson, G. Jönsson, B. Lindkvist, and A. Oskarsson, “The Disintegration of Nuclei in Violent Heavy Ion Interactions at $55A$ MeV– $110A$ MeV,” *Z. Phys. A* **307**, 293, (1982).
- [2] A. S. Botvina and I. N. Mishustin, “An Analysis of Multiplicity Dependence on Pseudorapidity Intervals at High Energy Collisions,” *Phys. Lett. B* **294**, 23 (1992).
- [3] J. P. Bondorf, A. S. Botvina, A. S. Iljinov, I. N. Mishustin, and K. Sneppen, “Statistical Multifragmentation of Nuclei,” *Phys. Rep.* **257**, 133 (1995).
- [4] *Isospin Physics in Heavy Ion Collisions at Intermediate Energies*, edited by Bao-An Li and W.Udo Schröder, ISBN 1-56072-888-4 (Nova Science, New York, 2001).
- [5] W. A. Friedman, “Are the Largest Products of Fragmentation Residues?” *Phys. Rev. C* **60**, 044603 (1999).
- [6] L. Pienkowski, K. Kwiatkowski, T. Lefort, W.-c. Hsi, L. Beaulieu, V. E. Viola, A. Botvina, R. G. Korteling, R. Laforest, E. Martin, E. Ramakrishnan, D. Rowland, A. Ruangma, E. Winchester, S. J. Yennello, B. Back, H. Breuer, S. Gushue, and L. P. Remsberg, “Breakup Time Scale Studied in the $8\text{ GeV}/c\pi^- + ^{197}\text{Au}$ Reaction,” *Phys. Rev. C* **65**, 064606 (2002).
- [7] H. Matsumura, K. Washiyama, H. Haba, Y. Miyamoto, Y. Oura, K. Sakamoto, S. Shibata, M. Furukawa, I. Fujiwara, H. Nagai, T. Kobayashi, and K. Kobayashi, “Target-Dependence of Light Fragment Production in Photonuclear Reactions at Intermediate Energies,” *Radiochim. Acta* **88**, 313 (2000).
- [8] V. K. Rodionov, S. P. Avdeyev, V. A. Karnaukhov, L. A. Petrov, V. V. Kirakosyan, P. A. Rukoyatkin, H. Oeschler, A. Budzanowski, W. Karcz, M. Janicki, O. V. Bochkarev, E. A. Kuzmin, L. V. Chulkov, E. Norbeck, and A. S. Botvina, “Time Scale of the Thermal Multifragmentation in $p + \text{Au}$ Collisions at 8.1 GeV ,” *Nucl. Phys. A* **700**, 457 (2002).
- [9] V. A. Karnaukhov, S. P. Avdeyev, E. V. Duginova, L. A. Petrov, V. K. Rodionov, H. Oeschler, A. Budzanowski, W. Karcz, M. Janicki, O. V. Bochkarev, E. A. Kuzmin, L. V. Chulkov, E. Norbeck, and A. S. Botvina, “Thermal Multifragmentation of Hot Nuclei and Liquid-Fog Phase Transition,” *Yad. Fiz.* **66**, 1282 (2003) [Phys. At. Nucl. **66**, 1242 (2003)].

- [10] M. B. Tsang, W. A. Friedman, C. K. Gelbke, W. G. Lynch, G. Verde, and H. S. Xu, “Isotopic Scaling in Nuclear Reactions,” Phys. Rev. Lett. **86**, 5023 (2001).
- [11] H. S. Xu, M. B. Tsang, T. X. Liu, X. D. Liu, W. G. Lynch, W. P. Tan, A. Vander Molen, G. Verde, A. Wagner, H. F. Xi, C. K. Gelbke, L. Beaulieu, B. Davin, Y. Larochelle, T. Lefort, R. T. de Souza, R. Yanez, V. E. Viola, R. J. Charity, and L. G. Sobotka “Isospin Fractionation in Nuclear Multifragmentation,” Phys. Rev. Lett. **85**, 716 (2000).
- [12] M. B. Tsang, C. K. Gelbke, X. D. Liu, W. G. Lynch, W. P. Tan, G. Verde, H. S. Xu, W. A. Friedman, R. Donangelo, S. R. Souza, C. B. Das, S. Das Gupta, and D. Zhabinsky, “Isoscaling in Statistical Models,” Phys. Rev. C **64**, 054615 (2001).
- [13] V. I. Bogatin, V. K. Bondarev, V. F. Litvin, O. V. Lozhkin, N. A. Perfilov, Yu. P. Yakovlev, and V. P. Bochin, “Investigation of Isotope Effects in Nuclear Reactions Induced by 660-MeV Protons,” Yad. Fiz. **19**, 32 (1974) [Sov. J. Nucl. Phys. **19**, 16 (1974)].
- [14] V. I. Bogatin, V. F. Litvin, O. V. Lozhkin, N. A. Perfilov, and Yu. P. Yakovlev, “Isotopic Effects in High-Energy Nuclear Reactions and Isospin Correlations of Fragmentation Cross Sections,” Nucl. Phys. **A260**, 446 (1976).
- [15] A. S. Botvina, O. V. Lozhkin, and W. Trautmann, “Isoscaling in Light-Ion Induced Reactions and Its Statistical Interpretation,” Phys. Rev. C **65**, 044610 (2002).
- [16] V. Aleksandryan, J. Adam, A. Balabekyan, A. S. Danagulyan, V. G. Kalinnikov, G. Musulmanbekov, V. K. Rodionov, V. I. Stegailov, and J. Frana, “Formation of Residual Nuclei with Medium Mass Number in the Reaction of Protons with Separated Tin Isotopes,” Nucl. Phys. **A674**, 539 (2000).
- [17] A. R. Balabekyan, A. S. Danagulyan, J. R. Drnoyan, N. A. Demekhina, J. Adam, V. G. Kalinnikov, and G. Musulmanbekov, “Isotopic Effects of Fragment-Yields in Proton Induced Reactions on Sn Isotopes,” Nucl. Phys. **A735**, 267 (2004).
- [18] A. R. Balabekyan, A. S. Danagulyan, J. R. Drnoyan, N. A. Demekhina, J. Adam, V. G. Kalinnikov, M. I. Krivopustov, V. S. Pronskikh, V. I. Stegailov, A. A. Solnishkin, P. Chaloun, V. M. Tsoupko-Sitnikov, and G. Musulmanbekov, “Investigation of Spallation Reactions on ^{120}Sn and (d, xn), (d, pxn), (p, xn), and (p, pxn) Reactions on Enriched Tin Isotopes,” Yad. Fiz. **68**, 195 (2005) [Phys. At. Nucl. **68**, 171 (2005)].
- [19] Ts. Damdinsuren, V. I. Iluschenko, P. Kozma, B. Tumendemberel, and D. Chultem, “Formation of Residues Nuclei in Interaction of 3.65A-GeV Deuterons with ^{93}Nb , ^{108}Ag , ^{159}Tb , ^{197}Au and $^{207.2}\text{Pb}$,” Yad. Fiz. **52**, 330 (1990) [Sov. J. Nucl. Phys. **52**, 209 (1990)]; JINR Preprint P1-89-757 (Dubna, 1989).
- [20] R. Michel, M. Gloris, H.-J. Lange, I. Leya, M. Lüpke, U. Herpers, B. Dittrich-Hannen, R. Rösel, Th. Sciek, D. Filges, P. Dragovitsch, M. Suter, H.-J. Hoffmann, W. Wölfl, P. W. Kubik, H. Bauer, and R. Wieler, “Nuclide Production by Proton-Induced Reactions on Elements ($6 \leq Z \leq 29$) in the Energy Range from 800 to 2600 MeV,” Nucl. Instrum. Methods Phys. Res. B **103**, 183 (1995).
- [21] A. Fassò, A. Ferrari, S. Roesler, P. R. Sala, F. Ballarini, A. Ottolenghi, G. Battistoni, F. Cerutti, E. Gadioli, M. V. Garzelli, A. Empl, and J. Ranft, “The Physics Models of FLUKA: Status and Recent Development,” E-print: hep-ph/0306267.

- [22] R. E. Prael and H. Lichtenstein, *User Guide to LCS: The LAHET Code System*, Los Alamos National Laboratory Report No. LA-UR-89-3014 (1989); <http://www-xdiv.lanl.gov/XTM/lcs/laht-doc.html>.
- [23] S. G. Mashnik, K. K. Gudima, I. V. Moskalenko, R. E. Prael, and A. J. Sierk, “CEM2k and LAQGSM Codes as Event Generators for Space-Radiation-Shielding and Cosmic-Ray-Propagation Applications,” *Advances in Space Research* **34**, 1288 (2004); E-print: [nucl-th/0210065](http://arxiv.org/abs/nucl-th/0210065).
- [24] R. Michel and P. Nagel, *International Code and Model Intercomparison for Intermediate Energy Activation Yields*, NSC/DOC(97)-1, NEA OECD, Paris, January 1997; <http://db.nea.fr/html/science/pt/ieay/>.